Biophysical Chemistry 137 (2008) 71–75

Contents lists available at ScienceDirect

Biophysical Chemistry

journal homepage: http://www.elsevier.com/locate/biophyschem

NMR studies on the surface accessibility of the archaeal protein Sso7d by using TEMPOL and Gd(III)(DTPA-BMA) as paramagnetic probes

Andrea Bernini [a], Vincenzo Venditti [a], Ottavia Spiga [a], Arianna Ciutti [a], Filippo Prischi [a], Roberto Consonni [b], Lucia Zetta [b], Ivana Arosio [b], Paola Fusi [c], Annamaria Guagliardi [d], Neri Niccolai [a,*]

[a] Università degli Studi di Siena, Dipartimento di Biologia Molecolare, via A. Fiorentina 1, 53100 Siena, Italy
[b] ISMAC Lab. NMR, CNR, via Bassini 15, 20133 Milano, Italy
[c] Dipartimento di Biotecnologie e Bioscienze, Università di Milano-Bicocca, P.zza della Scienza 2, 20126 Milano, Italy
[d] Dipartimento di Biologia Strutturale e Funzionale, Università Federico II, Via Cinthia 4, 80126, Napoli, Italy

ARTICLE INFO

Article history:
Received 10 June 2008
Received in revised form 8 July 2008
Accepted 8 July 2008
Available online 16 July 2008

Keywords:
Surface accessibility
Protein NMR
Paramagnetic probes
TEMPOL
Gd(III)(DTPA-BMA)

ABSTRACT

Understanding how proteins are approached by surrounding molecules is fundamental to increase our knowledge of life at atomic resolution. Here, the surface accessibility of a multifunctional small protein, the archaeal protein Sso7d from *Sulfolobus solfataricus*, has been investigated by using TEMPOL and Gd(III)(DTPA-BMA) as paramagnetic probes. The DNA binding domain of Sso7d appears very accessible both to TEMPOL and Gd(III)(DTPA-BMA). Differences in paramagnetic attenuation profiles of ^{1}H–^{15}N HSQC protein backbone amide correlations, observed in the presence of the latter paramagnetic probes, are consistent with the hydrogen bond acceptor capability of the *N*-oxyl moiety of TEMPOL to surface exposed Sso7d amide groups. By using the gadolinium complex as a paramagnetic probe a better agreement between Sso7d structural features and attenuation profile is achieved. It is interesting to note that the protein P-loop region, in spite of the high surface exposure predicted by the available protein structures, is not approached by TEMPOL and only partially by Gd(III)(DTPA-BMA).

1. Introduction

Molecular surface accessibility to paramagnetic probes, such as soluble nitroxide spin-labels [1–3], chelated complexes of Gd(III) ion [4] and molecular oxygen [5,6] has been extensively studied for proteins and RNAs. Absence of strong interactions of the latter probes with the investigated systems has been found and the observed paramagnetic perturbations of protein NMR signals have been interpreted in terms of structural features. A combined use of two paramagnetic probes with different size and chemical nature has been also proposed to increase the resolution of the paramagnetic perturbation approach and to delineate possible biased interactions between probes and proteins [4] or, conversely, to highlight common pathways of intermolecular approaches [7]. Enhanced accessibility of paramagnetic probes towards binding sites has been observed for the proteins so far investigated [8–11], offering important clues to understand how protein structure, dynamics and function are related. In this respect, the agreement with the results obtained with multiple solvent crystal structure (MSCS) studies [12] is remarkable. Organic solvents have been used to map protein accessibility also in solution [13] and the protein active site has been observed as the main target for unspecific interactions with molecules different than water.

For the interpretation of the available MSCS data, three conditions have been proposed for a protein surface patch to act as a binding site, being the presence of: i) local plasticity, ii) easily displaceable water molecules contributing to an entropically favorable component to binding and iii) hydrophobic surface hot spots. Particularly the latter two conditions could play a relevant role to drive paramagnetic probes towards specific protein surface regions.

The present report describes the combined use of two paramagnetic probes, TEMPOL and Gd(III)(DTPA-BMA), to map surface accessibility of Sso7d, a 62 residue protein from the extreme thermophilic crenarchaeon *Sulfolobus solfataricus* supporting multiple and structurally defined activities [14,15].

2. Materials and methods

2.1. Samples preparation

NMR samples of Sso7d were prepared by dissolving the protein in H2O/D2O (90:10, v/v) to make 1.2 mM and 1.0 mM solutions of the unlabeled and ^{15}N-enriched protein, respectively, always adjusted to pH 4.5 by addition of small amounts of HCl or KOH. No salt was added, to reproduce exactly the experimental conditions of the previous NMR

* Corresponding author. Tel.: +39 577234910; fax: +39 577234903.
E-mail address: niccolai@unisi.it (N. Niccolai).
URL: http://www.sbl.unisi.it (N. Niccolai).

0301-4622/$ – see front matter © 2008 Elsevier B.V. All rights reserved.
doi:10.1016/j.bpc.2008.07.003

studies on Sso7d. Procedures for protein expression and purification are reported elsewhere [16]. Paramagnetic NMR sample containing final probe concentrations of 18.0 and 1.2 mM respectively in the case of TEMPOL (Sigma-Aldrich) and Gd(III)(DTPA-BMA) (synthesis described in [8]) were obtained by addition of few microliters of 1.0 M TEMPOL or 10.0 M Gd(III)(DTPA-BMA) stock solutions; pH was carefully checked after probe additions. These probe concentrations yielded sizeable cross-peak attenuations in 2D spectra with a suitably good S/N.

2.2. NMR measurements

NMR measurements, run at 303 K, were performed on a Bruker DRX 600 spectrometer. Data processing was performed with the Bruker software and the spectral analysis with Sparky [17]. Water suppression was achieved following the scheme of Hwang [18]. The $^{1}H–^{15}N$ HSQC diamagnetic and paramagnetic spectra were obtained with 512 increments and 128 scans over 2048 data points. Observed chemical shifts were congruent with those from BioMagResBank (http://www.bmrb.wisc.edu) entry no. 5909, used for the assignment of ^{1}H and ^{15}N resonances.

A number n of well resolved NMR signals are compared by measuring cross-peak volumes in the presence and in the absence of the paramagnetic probes, respectively V_i^d and V_i^p. Such volumes have been measured with an estimated error lower than 10% and their autoscaled values, υ_i, were used according to the relation:

$$\upsilon_i^{p,d} = \frac{V_i^{p,d}}{(1/n)\sum_n V_i^{p,d}} \quad (1)$$

Paramagnetic attenuations, A_i, were calculated from the autoscaled diamagnetic and paramagnetic peak volumes, respectively, υ_d and υ_p, according to the relation:

$$A_i = 2 - \frac{\upsilon_i^p}{\upsilon_i^d} \quad (2)$$

2.3. Calculations of protein surface exposure and atom depth

Two minimized average Sso7d structures, available from the Protein Data Bank [19] for with the ID codes 1SSO and 1JIC, have been used as reference to discuss our data. Exposed surface areas and hydrogen bonding patterns have been calculated for backbone hydrogen atoms of Sso7d amide groups by using MolMol [20]. Surface exposed volumes, $ev_{i,n}$, of spheres of a suitable radius, r, centered on each of the i NH hydrogen atoms, have been calculated to have a measure of atom depths of Sso7d backbone amide groups [21]. In this way, atoms which are close to the protein surface exhibit large $ev_{i,r}$ values and *vice versa*. The largest radius of the probing sphere, which can be totally buried inside the protein structure, has to be chosen in order to obtain optimal dispersion of $ev_{i,r}$ values [21]. In the case of Sso7d this condition is met with a radius of 3 Å and, therefore, only $ev_{i,3}$ are discussed.

3. Results

3.1. Paramagnetic attenuation of $^{1}H–^{15}N$ HSQC signals

$^{1}H–^{15}N$ HSQC spectra of isotopically ^{15}N-enriched Sso7d have been recorded in the absence and in the presence of different concentrations of TEMPOL and Gd(III)(DTPA-BMA). As shown in Fig. 1, backbone amide correlations recorded in the $^{1}H–^{15}N$ HSQC spectra, obtained in the presence of 18.0 mM TEMPOL and 1.2 mM Gd(III)(DTPA-BMA), exhibit similar signal attenuations. The fact that Gd(III)(DTPA-BMA) and TEMPOL differ in i) electron spins, respectively 7/2 and 1/2,

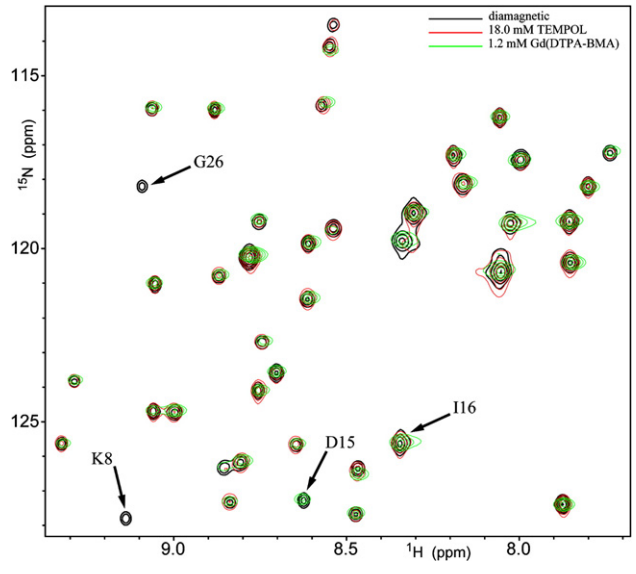

Fig. 1. Backbone amide region of $^{1}H–^{15}N$ HSQC spectra of isotopically ^{15}N-enriched Sso7d. $^{1}H–^{15}N$ HSQC signals, plotted with different colors depending on the absence (black contours) and the presence of TEMPOL (red contours) or Gd(III)(DTPA-BMA) (green contours). Arrows point to peaks exhibiting peculiar paramagnetic attenuations (see text). (For interpretation of the references to color in this figure legend, the reader is referred to the web version of this article.)

ii) electron spin relaxation rates [22,23] and iii) molecular reorientations, accounts for such a large difference in probe relaxivity. On a molar basis, indeed, Gd(III) complex induces much stronger signal attenuations than TEMPOL.

As a preliminary observation, from the data shown in Fig. 1 it is apparent that at the used probe concentrations no relevant ^{1}H and ^{15}N chemical shift changes can be detected. The fact that HSQC spectra recorded in the absence or in the presence of Gd(III)(DTPA-BMA) and TEMPOL are fully overlapping, confirms that no strong interactions between Sso7d and the used paramagnetic probes occur.

Paramagnetic attenuations induced by the presence in solution of TEMPOL and Gd(III)(DTPA-BMA), henceforth named A_{iT} and A_{iGd}, respectively, have been quantified for 53 well resolved Sso7d $^{1}H–^{15}N$ correlations out of the total 60 backbone amide signals. Standard deviations from the average for A_{iT} and A_{iGd} were $\sigma_T = 0.29$ and $\sigma_{Gd} = 0.18$, and in both cases only few attenuation values differ from the average $A_i = 1$ more than one σ unit. It is interesting to note that the two paramagnetic attenuation profiles shown in Fig. 2, in spite of the different size and chemical nature of the used paramagnets, exhibit a similar trend. In facts, only in the case of D15 amide signal, very attenuated by TEMPOL, the difference $A_{iT} - A_{iGd} = 1.10$ is much larger than the sum $\sigma_T + \sigma_{Gd}$. The strong paramagnetic perturbation experienced by K8, V22, G26 and K27 amide signals in the presence of both TEMPOL and Gd(III)(DTPA-BMA) is apparent, while I16 NH signal remains equally unperturbed by the two probes.

3.2. Surface accessibility of Sso7d backbone amides

Paramagnetic perturbations arise from through-space dipolar interactions between nuclear and unpaired electron spins. Thus, for the analysis of A_{iT} and A_{iGd} of each Sso7d NH hydrogen atom, depths rather than exposed areas should be considered. To account for possible scalar paramagnetic contributions, also exposed surface areas of protein backbone amides have been calculated and reported in Fig. 2. It should be noted that the two reference structures are rather similar, with a r.m.s.d calculated for all backbone atoms of 1.53. In particular, at the carboxy terminus and in the P-loop region the largest differences are found.

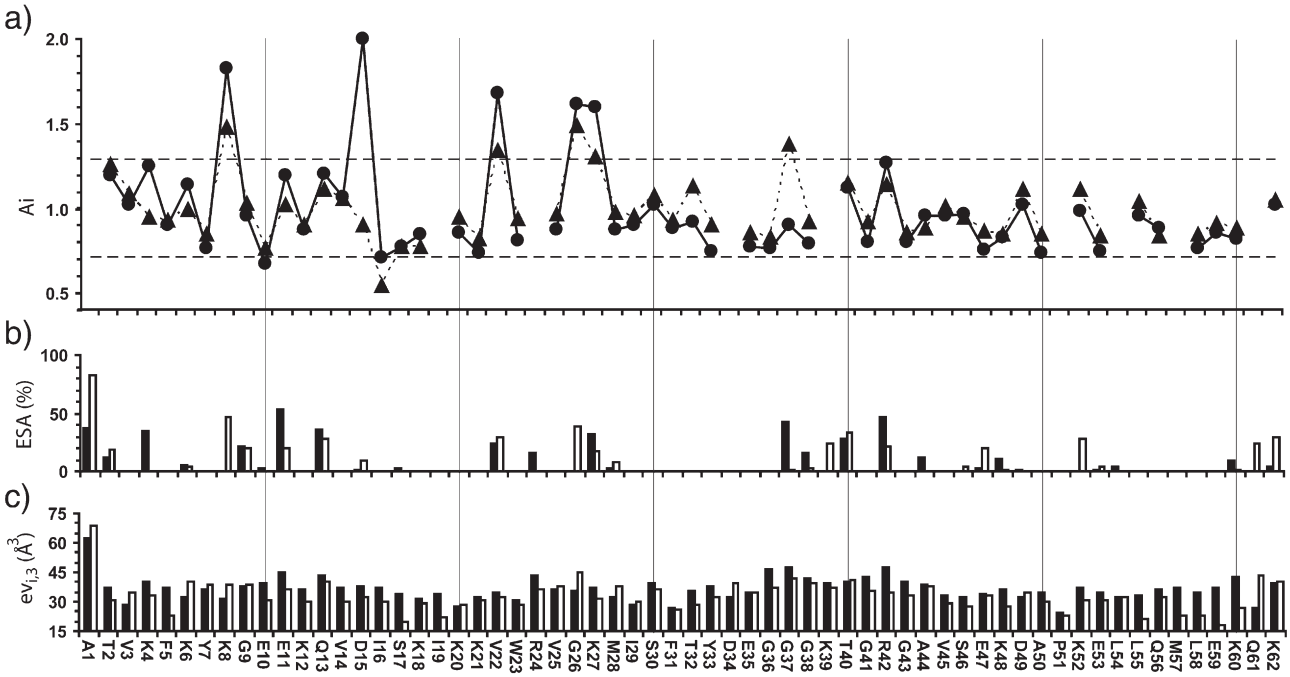

Fig. 2. Sequence dependence of experimental and calculated parameters of Sso7d backbone amides: a) paramagnetic attenuations (A_i) obtained by using TEMPOL (circles) and Gd(III)(DTPA-BMA) (triangles), with horizontal dashed lines plotted at the largest standard deviation value of A_i datasets; b) exposed surface areas of NH hydrogens calculated for the Sso7d structures with the PDB IDs 1SSO (white bars) and 1JIC (black bars); c) NH hydrogen depths expressed as exposed volumes calculated, as in b), on the basis of the two available protein structures.

The fact that the obtained profiles of atom depths and accessible surface areas are very different and hardly related, confirms that they have to be taken separately into account. It is apparent, indeed, that a given backbone atom can be very close to the protein van der Waals surface and, therefore, very exposed to the paramagnetic perturbation, but, at the same time, totally buried by surrounding protein side chains.

4. Discussion

From a preliminary overview of the paramagnetic perturbations experienced by HSQC amide signals of Sso7d, once 18.0 mM TEMPOL or 1.2 mM Gd(III)(DTPA-BMA) are added to the protein aqueous solution, strong paramagnet–protein interactions can be ruled out. This prerequisite of any potential accessibility probe is fulfilled, since no sizeable chemical shift changes or total signal disappearance has been detected. Then, it should be noted also that the small size and the shape of Sso7d cannot ensure, even for protein inner atoms, enough protection from long-distance and through-space perturbations due to the presence in solution of TEMPOL and Gd(III)(DTPA-BMA). This feature explains the reason why most of the backbone amide signals of Sso7d experience average paramagnetic attenuations. In facts, for each of the 53 analyzed signals, the respective A_{iT} or A_{iGd} value lies above one standard deviation unit from the average only for six amino acids and below it for two amino acids (K8, D15, V22, G26, K27, G37 and E10, I16, respectively). However, among these cases two inconsistencies are present, as $A_{iT} >> A_{iGd}$ is found for D15 NH group, while the $A_{iT} << A_{iGd}$ condition holds for G37 amide.

To explain the first anomalous A_i value, the formation of an intermolecular hydrogen bonding between D15 amide and TEMPOL *N*-oxyl group can be invoked. This H-bond, weak enough not to induce detectable chemical shift, is in principle possible, due to partial protein surface exposure of the donor D15 NH group (see Fig. 2b), free from intramolecular H-bonds in both reference structures. Furthermore, the

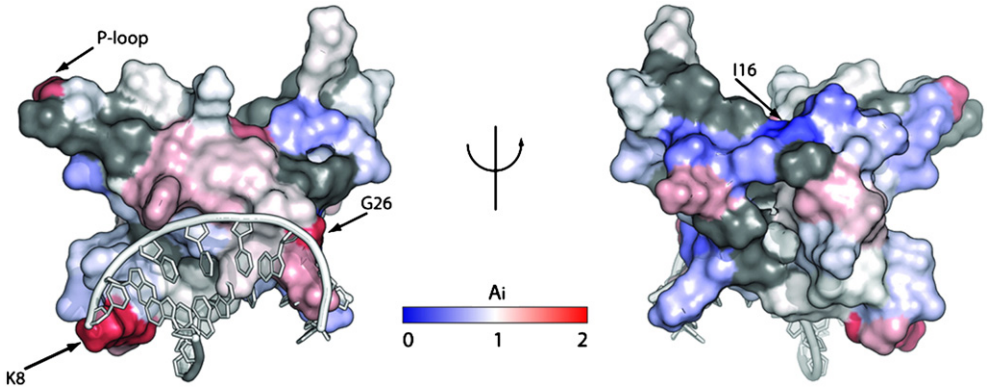

Fig. 3. Surface representation of Sso7d colored according to the paramagnetic attenuation induced by Gd(III)(DTPA-BMA) (low, average and high attenuations are reported as blue, white and red colors, respectively, see color bar; residues without attenuation data were grayed out). The crystal structure of Sso7d/DNA complex from PDB file 1BF4 was used to highlight the attenuation profile of the DNA binding site. Large and extended attenuation is experienced particularly by the H-bond free residues K8 and G26 mainly involved in the interaction with DNA. (For interpretation of the references to color in this figure legend, the reader is referred to the web version of this article.)

acceptor capability of nitroxide *N*-oxyl group to form weak hydrogen bonding with amide moieties has been recently confirmed [24]. It should be noted also that hydrogen bonding of this protein moiety with acidic side chain groups has been recently excluded [25].

The fact that surface exposed and H-bond available amides of protein backbone have been proposed as relevant sites for intermolecular interactions [26] is consistent with the possibility of an interaction between the N7 atom of the ATP purine ring and the D15 amide group. The latter hypothesis is in agreement also with the structure of the ATP–Sso7d complex which has been predicted from docking simulation [14]. A relevant role of hydrogen bonding between TEMPOL *N*-oxyl oxygen and protein backbone NH hydrogens in determining the extent of paramagnetic perturbations is confirmed also by the fact that the condition $A_{iT} > 1.29$ is met only by amide groups which are fully available to intermolecular interactions both in 1SSO and 1JIC structures.

Large discrepancy between A_{iT} and A_{iGd} values is observed for G37 NH correlation. Conformational exchange of the protein loop where G37 is located, suggested by the different orientations of G37 amide observed in the two Sso7d reference structures, can be responsible of a reduced life-time of intermolecular H-bonds of G37 NH with solvent and nitroxide molecules. However, in both reference structures G37 amide group is very close to the surface, see Fig. 2c, and the lack of a bulky side chain in the glycyl residue can favor short distance approaches between Gd(III)(DTPA-BMA) and G37 NH hydrogen.

As shown in Fig. 2, both TEMPOL and Gd(III)(DTPA-BMA) induce strong paramagnetic attenuations for the NH correlations of K8, G26 and K27, indicating that the protein–DNA interface, where all these H-bond free amide groups are located, exhibits an overall enhanced surface accessibility, see Fig. 3. For this surface region, which is also involved in the Sso7d chaperone activity [14], confirmed the already observed preferential access of soluble neutral paramagnets towards protein active sites [7–9,27]. However, this is not the case of glycyl 36–38 fragment, located in the center of the protein P-loop region and responsible for the Sso7d ATPase activity. This protein active site, in spite of the high surface exposure predicted by both reference structures, appears shielded from intermolecular interactions with the used paramagnets, since only G37 amide signal in the presence of Gd(III)(DTPA-BMA) experiences high paramagnetic attenuation. This finding is rather anomalous, as binding sites have been always observed as preferred targets of paramagnetic probes. Reduced mobility of water molecules in this area could be responsible of the anomalous surface accessibility observed for Sso7d P-loop. Enhanced stability of the hydration shell near to the amino group of Lys39 side chain, the active site for the interaction with ATP, can be responsible of the observed hindered approach of both paramagnets, in order to preserve Sso7d P-loop from unspecific intermolecular interactions.

The obtained high A_{iT} and A_{iGd} values of V22 NH correlation are consistent with the surface exposure of this amide group, which is also available for intermolecular hydrogen bonding. A surface hot spot, whose functional role is not yet defined, is delineated for the latter Sso7d moiety, far from both DNA and ATP binding sites. The lowest A_{iT} and A_{iGd} value observed for the I16 amide correlation is consistent with the buried position of this group in the protein structure (see Figs. 2 and 3). A further protection from the probe access seems to be due to the hindrance of the bulky isoleucyl side chain.

As a concluding remark, it should be stressed that a combined use of TEMPOL and Gd(III)(DTPA-BMA) as paramagnetic probes in $^{1}H–^{15}N$ HSQC spectroscopy gives the unique opportunity to study the distribution on the protein surface of donor amide groups for intermolecular H-bonds. The $A_{iT} >> Ai_{Gd}$ condition is, indeed, diagnostic of a very important feature, since these amides are frequently found in protein binding sites [26] and/or at the interface of interacting proteins [28,29]. Finally, the fact that the $A_{iGd} > A_{iT}$ condition holds for all the Sso7d glycyl residues, suggests a relevant role of amino acid side chain size in determining the extent of Gd(III)(DTPA-BMA) paramagnetic perturbation of surface exposed regions of protein backbone.

Acknowledgement

Thanks are due to the University of Siena for financial support.

References

[1] H. Molinari, G. Esposito, L. Ragona, M. Pegna, N. Niccolai, R.M. Brunne, A.M. Lesk, L. Zetta, Probing protein structure by solvent perturbation of NMR spectra: the surface accessibility of bovine pancreatic trypsin inhibitor, Biophys J 73 (1997) 382–396.
[2] G. Esposito, A.M. Lesk, H. Molinari, A. Motta, N. Niccolai, A. Pastore, Probing protein structure by solvent perturbation of nuclear magnetic resonance spectra. Nuclear magnetic resonance spectral editing and topological mapping in proteins by paramagnetic relaxation filtering, J Mol Biol 224 (1992) 659–670.
[3] V. Venditti, N. Niccolai, S.E. Butcher, Measuring the dynamic surface accessibility of RNA with the small paramagnetic molecule TEMPOL, Nucleic Acids Res 36 (2007) e20.
[4] G. Pintacuda, G. Otting, Identification of protein surfaces by NMR measurements with a paramagnetic Gd(III) chelate, J Am Chem Soc 124 (2002) 372–373.
[5] C.L. Teng, R.G. Bryant, Mapping oxygen accessibility to ribonuclease a using high-resolution NMR relaxation spectroscopy, Biophys J 86 (2004) 1713–1725.
[6] C.L. Teng, B. Hinderliter, R.G. Bryant, Oxygen accessibility to ribonuclease a: quantitative interpretation of nuclear spin relaxation induced by a freely diffusing paramagnet, J Phys Chem A Mol Spectrosc Kinet Environ Gen Theory 110 (2006) 580–588.
[7] A. Bernini, O. Spiga, V. Venditti, F. Prischi, L. Bracci, A.P. Tong, W.T. Wong, N. Niccolai, NMR studies of lysozyme surface accessibility by using different paramagnetic relaxation probes, J Am Chem Soc 128 (2006) 9290–9291.
[8] A. Bernini, O. Spiga, A. Ciutti, V. Venditti, F. Prischi, M. Governatori, L. Bracci, B. Lelli, S. Pileri, M. Botta, A. Barge, F. Laschi, N. Niccolai, NMR studies of BPTI aggregation by using paramagnetic relaxation reagents, Biochim Biophys Acta 1764 (2006) 856–862.
[9] N. Niccolai, O. Spiga, A. Bernini, M. Scarselli, A. Ciutti, I. Fiaschi, S. Chiellini, H. Molinari, P.A. Temussi, NMR studies of protein hydration and TEMPOL accessibility, J Mol Biol 332 (2003) 437–447.
[10] M. Scarselli, A. Bernini, C. Segoni, H. Molinari, G. Esposito, A.M. Lesk, F. Laschi, P. Temussi, N. Niccolai, Tendamistat surface accessibility to the TEMPOL paramagnetic probe, J Biomol NMR 15 (1999) 125–133.
[11] V. Venditti, A. Bernini, A. De Simone, O. Spiga, F. Prischi, N. Niccolai, MD and NMR studies of alpha-bungarotoxin surface accessibility, Biochem Biophys Res Commun 356 (2007) 114–117.
[12] C. Mattos, C.R. Bellamacina, E. Peisach, A. Pereira, D. Vitkup, G.A. Petsko, D. Ringe, Multiple solvent crystal structures: probing binding sites, plasticity and hydration, J Mol Biol 357 (2006) 1471–1482.
[13] C. Dalvit, P. Floersheim, M. Zurini, A. Widmer, Use of organic solvents and small molecules for locating binding sites on proteins in solutions, J Biomol NMR 14 (1999) 23–32.
[14] G. Renzone, R.M. Vitale, A. Scaloni, M. Rossi, P. Amodeo, A. Guagliardi, Structural characterization of the functional regions in the archaeal protein Sso7d, Proteins 67 (2007) 189–197.
[15] R. Consonni, I. Arosio, T. Recca, P. Fusi, L. Zetta, Structural determinants responsible for the thermostability of Sso7d and its single point mutants, Proteins 67 (2007) 766–775.
[16] P. Fusi, M. Grisa, E. Mombelli, R. Consonni, P. Tortora, M. Vanoni, Expression of a synthetic gene encoding P2 ribonuclease from the extreme thermoacidophilic archaebacterium *Sulfolobus solfataricus* in mesophylic hosts, Gene 154 (1995) 99–103.
[17] T.D. Goddard and D.G. Kneller, SPARKY 3, University of California, San Francisco.
[18] T. Hwang, A.J. Shaka, Water suppression that works. Excitation sculpting using arbitrary waveforms and pulsed field gradients, J Magn Reson Ser A 112 (1995) 275–279.
[19] H. Berman, K. Henrick, H. Nakamura, J.L. Markley, The worldwide Protein Data Bank (wwPDB): ensuring a single, uniform archive of PDB data, Nucleic Acids Res 35 (2007) D301–D303.
[20] R. Koradi, M. Billeter and K. Wuthrich, MOLMOL: a program for display and analysis of macromolecular structures, Journal of Molecular Graphics 14 (1996) 51–55, 29–32.
[21] D. Varrazzo, A. Bernini, O. Spiga, A. Ciutti, S. Chiellini, V. Venditti, L. Bracci, N. Niccolai, Three-dimensional computation of atom depth in complex molecular structures, Bioinformatics 21 (2005) 2856–2860.
[22] D.H. Powell, O.M.N. Dhubhghaill, D. Pubanz, L. Helm, Y.S. Lebedev, W. Schlaepfer, A.E. Merbach, Structural and dynamic parameters obtained from 17O NMR, EPR, and NMRD studies of monomeric and dimeric Gd3+ complexes of interest in magnetic resonance imaging: an integrated and theoretically self-consistent approach, JACS 118 (1996) 9333–9346.
[23] I. Panagiotelis, I. Nicholson, J.M. Hutchison, Electron spin relaxation time measurements using radiofrequency longitudinally detected ESR and application in oximetry, J Magn Reson 149 (2001) 74–84.
[24] J.L. Russ, J. Gu, K.H. Tsai, T. Glass, J.C. Duchamp, H.C. Dorn, Nitroxide/substrate weak hydrogen bonding: attitude and dynamics of collisions in solution, J Am Chem Soc 129 (2007) 7018–7027.

[25] A.T. Clark, K. Smith, R. Muhandiram, S.P. Edmondson, J.W. Shriver, Carboxyl pK(a) values, ion pairs, hydrogen bonding, and the pH-dependence of folding the hyperthermophile proteins Sac7d and Sso7d, J Mol Biol 372 (2007) 992–1008.
[26] D. Ringe, What makes a binding site a binding site? Curr Opin Struct Biol 5 (1995) 825–829.
[27] N. Niccolai, A. Ciutti, O. Spiga, M. Scarselli, A. Bernini, L. Bracci, D. Di Maro, C. Dalvit, H. Molinari, G. Esposito, P.A. Temussi, NMR studies of protein surface accessibility, J Biol Chem 276 (2001) 42455–42461.
[28] A. De Simone, G.G. Dodson, C.S. Verma, A. Zagari, F. Fraternali, Prion and water: tight and dynamical hydration sites have a key role in structural stability, Proc Natl Acad Sci U S A 102 (2005) 7535–7540.
[29] A. De Simone, R. Spadaccini, P.A. Temussi, F. Fraternali, Toward the understanding of MNEI sweetness from hydration map surfaces, Biophys J 90 (2006) 3052–3061.